

Positron–Hydrogen Scattering at Intermediate Energies

Jim Mitroy

Faculty of Science, Northern Territory University,
Darwin, NT 0909, Australia.

Abstract

Calculations of positron–hydrogen scattering at intermediate energies up to a maximum energy of 10 Ryd are performed using the close coupling (CC) approach. A large L^2 basis of positron–hydrogen channels (28 states) is supplemented by the $Ps(1s)$, $Ps(2s)$ and $Ps(2p)$ channels. The inclusion of the positronium states in the CC expansion leads to a model which can describe most of the physics of the positron–hydrogen system with a reasonable degree of accuracy. In particular, the positronium formation cross section, the total reaction cross section and the ionisation cross section are all in agreement with experiment. The elastic scattering cross section and the cross sections for positron impact excitation of the $H(2s)$ and $H(2p)$ levels are also reported.

1. Introduction

The Coulomb three-body system is an example of a physical system of beguiling simplicity but fraught with formidable problems of both a practical and formal nature. The chief source of difficulty concerns the long range nature of the Coulomb interaction. When it comes to performing precise calculations, it seems to be the case that the difficulties associated with the Coulomb interaction increase as the total energy of the system increases. At low energies, where the three particles can often combine to form a bound state, it is possible to perform calculations of very high accuracy as exemplified by calculations performed on the helium atom. Things have reached such a state of refinement that the precision of the best calculations exceeds the precision of the best experiments (Pekeris 1959; Drake 1993). The next region of interest is the energy region for which the three-body system can exist as a two-body bound state plus one particle in the continuum. Two of the more important three-body scattering systems are the electron–hydrogen and positron–hydrogen systems. Scattering calculations are almost always more difficult than calculations for bound-state systems and progress in the area of positron–hydrogen scattering has been steady, if not spectacular for the last two decades. A number of different groups have gradually increased the accuracy and range of validity of the calculations (Bhatia *et al.* 1971, 1974; Brown and Humberston 1985; Humberston 1982, 1984). Recently, the development of improved theoretical procedures coupled with the availability of faster computers has resulted in a spurt of calculations for the low energy region (Archer *et al.* 1990; Igarashi and Toshima 1994; Mitroy 1993*b*, 1995; Mitroy

et al. 1994; Mitroy and Ratnavelu 1995; Zhou and Lin 1994, 1995). The most difficult energy region is undoubtedly the region in which three-body breakup reactions are possible. A major achievement has been the demonstration that physical observables for electron–hydrogen scattering in the intermediate energy region appear to converge in close coupling (CC) calculations with a very large pseudo-state basis (Bray and Stelbovics 1992, 1993).

Besides the difficulties associated with the Coulomb interaction, there is another source of trouble which further complicates the analysis in the case of the positron–hydrogen system. For a total three-body energy with $E \geq 0.5$ Ryd, it is possible to form two different two-body bound state systems. These are the hydrogen bound states and the positronium bound states. Having two different manifolds of possible bound states leads to two sets of difficulties. Firstly, from a pragmatic viewpoint, the matrix elements connecting the two different manifolds of channels are much more complicated than those arising in electron–hydrogen calculations. Only in the last three years have CC calculations with even a limited number of positronium channels become routine (Mitroy 1993*a*; McAlinden *et al.* 1994). The other difficulty is more fundamental and arises from the fact that two different manifolds of states need to be included in the CC expansion. If both sets of states are expanded towards completeness, then the degree of linear dependence will increase and this could lead to numerical instabilities (Bransden and Noble 1994). Numerical instabilities of a minor nature have been observed in a large basis calculation of positron–hydrogen scattering (Mitroy 1995).

When it comes to positron–hydrogen scattering in the intermediate energy region, there has been a scarcity of calculations which are expected to give a realistic description of the dynamics of positron–hydrogen scattering. There have been some calculations that used a large pseudo-state basis of positron–hydrogen states in an attempt to represent the ionisation continuum (Winick and Reinhardt 1978*b*; Higgins *et al.* 1990; Bray and Stelbovics 1994; Walters 1988). However, these calculations did not allow for positronium formation and it is doubtful whether these calculations are accurate in the energy region where the positronium formation cross section is the largest cross section. Just recently, there have been some calculations that have explicitly allowed for the coupling between the hydrogen and positronium states (Hewitt *et al.* 1990; Mitroy and Stelbovics 1994*b*, 1994*c*; McAlinden *et al.* 1994; Sarkar and Ghosh 1994), however, for the most part the size of the channel space has been relatively small. One of the features of these calculations was the presence of numerous resonances above the ionisation threshold (Higgins and Burke 1991; Kernoghan *et al.* 1994; Mitroy and Stelbovics 1994*a*). Most recently, the *R*-matrix method (Kernoghan *et al.* 1995) was used in the first serious attempt to explicitly include both the ionisation continuum and the positronium formation channels in a calculation in the intermediate energy region. Although, there are some serious questions relating to the interpretation of the *R*-matrix calculation, this work did result in a set of cross sections which were a lot closer to experiment than previous calculations.

In this paper, the results of a CC calculation of positron–hydrogen scattering in which a large L^2 basis of hydrogen states has been supplemented by the lowest lying positronium states are reported. The large basis of hydrogen states were included in order to have an adequate representation of the ionisation continuum. The low-lying $Ps(1s)$, $Ps(2s)$ and $Ps(2p)$ states were included in the calculation

since the positronium formation cross section is the largest cross section for $E < 3.0$ Ryd. Since all the states that could couple with any strength to the $e^+ - H(1s)$ entrance channel have been included, it is anticipated that the present model will do a reasonable job of modelling the physics of positron-hydrogen scattering. An abbreviated version of the present calculation has recently been published (Mitroy 1996).

2. Theoretical Details

The calculations reported in this article are based upon the techniques used in previous calculations of electron-hydrogen and positron-hydrogen scattering with some minor modifications (McCarthy and Stelbovics 1983; Mitroy 1993a). Therefore, the discussion will be confined to those aspects of the calculation which are different from previous calculations. The CC equations are written in terms of a set of coupled Lippmann-Schwinger type integral equations. However, rather than solving an integral equation for the T -matrix, an integral equation has been solved for the K -matrix. Using the K -matrix rather than the T -matrix permits the most memory intensive aspect of the calculation, i.e. the solution of the linear equations, to be performed in real as opposed to complex arithmetic. (In practice, the solution of the linear equations was performed in double precision arithmetic.) Since linear equations of order 3000 – 4000 need to be solved, it is desirable to minimise the memory requirements.

The integral equations for a positron with momentum \mathbf{k} incident upon a hydrogen atom in state Ψ_α are

$$\begin{aligned} \langle \mathbf{k}' \Psi_{\alpha'} | K | \mathbf{k} \Psi_\alpha \rangle &= \langle \mathbf{k}' \Psi_{\alpha'} | V | \mathbf{k} \Psi_\alpha \rangle \\ &+ \sum_{\alpha''} P \int d^3 k'' \frac{\langle \mathbf{k}' \Psi_{\alpha'} | V | \mathbf{k}'' \Psi_{\alpha''} \rangle \langle \mathbf{k}'' \Psi_{\alpha''} | K | \mathbf{k} \Psi_\alpha \rangle}{(E - \epsilon_{\alpha''} - \frac{1}{2} k''^2)} \\ &+ \sum_{\beta''} P \int d^3 k'' \frac{\langle \mathbf{k}' \Psi_{\alpha'} | V | \mathbf{k}'' \Phi_{\beta''} \rangle \langle \mathbf{k}'' \Phi_{\beta''} | K | \mathbf{k} \Psi_\alpha \rangle}{(E - \epsilon_{\beta''} - \frac{1}{4} k''^2)}, \end{aligned}$$

$$\begin{aligned} \langle \mathbf{k}' \Phi_{\beta'} | K | \mathbf{k} \Psi_\alpha \rangle &= \langle \mathbf{k}' \Phi_{\beta'} | V | \mathbf{k} \Psi_\alpha \rangle \\ &+ \sum_{\alpha''} P \int d^3 k'' \frac{\langle \mathbf{k}' \Phi_{\beta'} | V | \mathbf{k}'' \Psi_{\alpha''} \rangle \langle \mathbf{k}'' \Psi_{\alpha''} | K | \mathbf{k} \Psi_\alpha \rangle}{(E - \epsilon_{\alpha''} - \frac{1}{2} k''^2)} \\ &+ \sum_{\beta''} P \int d^3 k'' \frac{\langle \mathbf{k}' \Phi_{\beta'} | V | \mathbf{k}'' \Phi_{\beta''} \rangle \langle \mathbf{k}'' \Phi_{\beta''} | K | \mathbf{k} \Psi_\alpha \rangle}{(E - \epsilon_{\beta''} - \frac{1}{4} k''^2)}, \end{aligned}$$

$$\begin{aligned} \langle \mathbf{k}' \Phi_{\beta'} | K | \mathbf{k} \Phi_{\beta} \rangle &= \langle \mathbf{k}' \Phi_{\beta'} | V | \mathbf{k} \Phi_{\beta} \rangle \\ &+ \sum_{\alpha''} P \int d^3 k'' \frac{\langle \mathbf{k}' \Phi_{\beta'} | V | \mathbf{k}'' \Psi_{\alpha''} \rangle \langle \mathbf{k}'' \Psi_{\alpha''} | K | \mathbf{k} \Phi_{\beta} \rangle}{(E - \epsilon_{\alpha''} - \frac{1}{2} k''^2)} \\ &+ \sum_{\beta''} P \int d^3 k'' \frac{\langle \mathbf{k}' \Phi_{\beta'} | V | \mathbf{k}'' \Phi_{\beta''} \rangle \langle \mathbf{k}'' \Phi_{\beta''} | K | \mathbf{k} \Phi_{\beta} \rangle}{(E - \epsilon_{\beta''} - \frac{1}{4} k''^2)} \end{aligned}$$

In the set of equations above, V labels the interactions between the different classes of channels, and Ψ_{α} and Φ_{β} denote the hydrogen and positronium states respectively. It is necessary to solve the integral equation for all possible entrance channels. Once the full K -matrix has been obtained, the T -matrix is easily obtained from just the on-shell values. The numerical procedures involved in solving the Lippmann–Schwinger equation for the K -matrix are almost identical to those needed for the T -matrix. It was a relatively minor operation to convert the existing T -matrix program to solve for the K -matrix.

The principal value integral is performed by using an on-shell subtraction (McCarthy and Stelbovics 1983). For calculations with a lot of different channels, the use of the same quadrature rule for the k'' integral for each intermediate state has problems. Since there will be roughly 30 different on-shell momenta, it is almost certain that some of the off-shell k'' quadrature points will lie close to the singularity for some of the channels. When this occurs, the principal value subtraction is subject to large cancellations and the precision of the final result is degraded. This potential source of inaccuracy was eliminated by using a different quadrature rule for each intermediate state. With a different quadrature rule for each channel, it was always possible to tune the grid parameters so that

$$P \int_0^{\infty} dk'' \frac{k''^2}{(E - \epsilon_{\alpha''} - \frac{1}{2} k''^2)} = \sum_i \frac{w_i k_i''^2}{(E - \epsilon_{\alpha''} - \frac{1}{2} k_i''^2)} = 0$$

is zero for a particular set of quadrature abscissas and weights. The equality to zero was enforced by expressing the on-shell weight as a function of the parameters used to tune the mesh and solving a non-linear equation. In practice, the principal value subtraction for the different channels was not exactly zero and was of the order of 10^{-10} .

The individual states are written in terms of a linear superposition of Laguerre functions. The specific definition of the Laguerre functions is

$$\chi_{kl}(r) = \sqrt{\frac{\lambda(k-1)!}{(2l+1+k)!}} (\lambda r)^{l+1} \exp(-\frac{1}{2}\lambda r) L_{k-1}^{2l+2}(\lambda r).$$

In this expression, the $L_{k-1}^{2l+2}(\lambda r)$ are Laguerre polynomials.

The physical and pseudo-state hydrogen orbitals were computed by diagonalising the hydrogen Hamiltonian with respect to the Laguerre basis. Since only a couple of positronium states are included in the calculation, the Laguerre representation for these states was specifically chosen to generate the exact eigenstates in a

minimal length expansion. While the hydrogen and positronium states have an analytic representation, this has not been exploited during the calculation. All the momentum space form factors needed during the course of the calculation have been computed by performing the Fourier transforms numerically.

In the present work a total of $11s$, $9p$ and $8d$ states were included in the L^2 expansion of the hydrogen levels. A value of $\lambda = 2.0$ was adopted for the exponent of the Laguerre basis for $l = 0, 1$ and 2 . In order to get accurate representations of the $H(2s)$ and $H(2p)$ states while keeping the size of the basis down, the basis was contracted after diagonalisation. For the $l = 0$ states, the raw basis contained 13 Laguerre functions, and the lowest 11 states were retained after diagonalisation. The $l = 1$ states were constructed from a raw basis of 11 Laguerre functions, and the $l = 2$ states were constructed from a basis of 10 Laguerre functions.

The simultaneous inclusion of a large L^2 set of positronium type states is problematic for two reasons. First, if a complete set of positronium and hydrogen type channels is included, the basis could become over-complete and this could cause linear dependence problems when attempting to solve the Lippmann-Schwinger equations (Bransden and Noble 1994; Stelbovics and Berge 1996). The second is more pragmatic, as a larger calculation would have been beyond the scope of the available computing resources (a DEC 3000/800S workstation). As it was, the present calculations used almost 400 MByte of RAM memory, created scratch disk files totalling 5 Gbytes, and took 2-5 days to complete depending on the energy.

The calculations for which results are reported in this work are labelled by the $CC(m, n)$ notation adopted in previous works (Mitroy 1993a, 1995). The m and n refer to the number of hydrogenic and positronium states included in the CC calculation. A basis with a significant number of pseudo-states is represented by putting a bar over the m or n . The following calculations were performed:

$CC(\overline{28}, 0)$. In this calculation the 28 hydrogen states described above were included and no consideration was given to positronium formation. In some respects, this calculation has similarities with the moment T -matrix method (MTM) calculation (Winick and Reinhardt 1978a, 1978b), the intermediate energy R -matrix (IERM) calculation (Higgins *et al.* 1990) and the convergent close coupling (CCC) calculation (Bray and Stelbovics 1994). These other calculations used a more extensive L^2 basis than the present calculation. The CCC calculation included states with $l = 3$ and the IERM calculation performed an extrapolation to simulate a basis of infinite size.

$CC(\overline{28}, 1)$. Except for the inclusion of the $Ps(1s)$ level into the calculation, this calculation was exactly the same as the $CC(\overline{28}, 0)$ calculation. Some account of the Ps formation process has to be made since this cross section is the largest cross section for $E < 3$ Ryd.

$CC(\overline{28}, 3)$. In this case the $Ps(1s)$, $Ps(2s)$ and $Ps(2p)$ states were added to the basis. The inclusion of the additional positronium states was motivated by the knowledge that the $Ps(2s)$ and $Ps(2p)$ states can contribute 30% to the Ps formation cross section at energies above 2 Ryd (Mitroy and Stelbovics 1994b). Computational constraints prevented additional positronium states being included in the calculation.

Besides the calculations performed for this work, comparison will be made to earlier calculations of the CC type. These include:

$CC(3, 3)$. This is the simplest possible model of the positron–hydrogen system that can be regarded as realistic. It includes the $H(1s)$, $H(2s)$, $H(2p)$, $Ps(1s)$, $Ps(2s)$ and $Ps(2p)$ states. Two groups have computed reliable cross sections with this model (McAlinden *et al.* 1994; Mitroy and Stelbovics 1994*b*, 1994*c*).

$CC(\bar{9}, \bar{9})$. This contains a total of 3 physical and 6 pseudo-hydrogen states. The positronium states were identical to the hydrogen states when the different reduced mass was taken into account. The R -matrix method has been used to compute cross sections with this model (McAlinden *et al.* 1994; Kernoghan *et al.* 1994, 1995).

$CC(\bar{13}, \bar{8})$. This is the most accurate of the models used for the low energy CC calculations. It is expected to have an accuracy of better than 2% for most cross sections (Mitroy 1995).

The integral equations had to be discretised on a large quadrature mesh including up to 70 discrete momenta in order to ensure the T -matrix elements were reliable. One way to assess the numerical accuracy of the present calculations is to examine the energy dependence of the $CC(\bar{28}, 0)$ cross sections as a function of energy. [Using the $CC(\bar{28}, 3)$ cross sections to assess the quality of the quadrature mesh is more problematic since resonant structures are present in the cross section.] Since the calculations at different energies are completely different, any problems with the numerical grid would result in cross sections that did not have a smooth energy dependence. A visual examination of Figs 1 to 6 below does not reveal any irregularities in the energy dependence of the $CC(\bar{28}, 0)$ cross sections that can be attributed to numerical factors. Cross sections for the $CC(\bar{28}, 0)$, $CC(\bar{28}, 1)$ and $CC(\bar{28}, 3)$ models are only depicted for incident positron energies greater than or equal to 1 Ryd in Figs 1 to 6. Some calculations have been performed at energies below the ionisation threshold for validation purposes, however, the resulting cross sections are only presented in tabular form.

The CC equations were solved up to a maximum angular momentum (J) of 16 at an incident energy of 1 Ryd. This value was increased to 36 at an incident energy of 10.0 Ryd. The rearrangement kernel was included in the solution of the CC equations for $J \leq 14$. Small corrections were made to all the cross sections by assuming that the omitted portion of the partial wave sum scaled like a geometric series. The largest correction occurred for the $H(2p)$ dipole excitation and the maximum size of the correction was always less than 7%. Cross sections were computed in energy increments of 0.1–0.5 Ryd with smaller energy steps being used at the lower energies. All the graphs were drawn by using linear interpolation to connect the discrete set of points.

3. Validation at Low Energies

An indication of the ability of the particular CC expansions used in this work to accurately describe the physics of positron–hydrogen scattering can be determined by doing some initial calculations in the low energy region. There have been a number of high precision calculations at incident positron energies below the positronium formation threshold and in the Ore gap which are expected to give cross sections that are accurate to within 1% or 2% (Bhatia *et al.* 1971, 1974; Brown and Humberston 1985; Humberston 1982, 1984; Mitroy 1995; Mitroy *et al.* 1994).

Phase shifts for the $J = 0, 1, 2$ and 3 partial waves are given for a number of different model calculations in Table 1 and compared with previous variational and $CC(\bar{13}, \bar{8})$ model phase shifts. The variational and $CC(\bar{13}, \bar{8})$ phase shifts are expected to be close to the exact phase shifts. The $CC(\bar{28}, 0)$ calculation does a poor job of reproducing these phase shifts. The s-wave phase shift underestimates the exact phase shift by 0.06 rad and the p-wave phase is too small by 0.03 rad. There is a marked improvement for the $CC(\bar{28}, 1)$ basis which contains the $Ps(1s)$ state. The maximum error for this model occurs for the s-wave and is less than 0.01 rad. This provides dramatic evidence that the very slow convergence noticed in previous single-centre coupling calculations (McEachran and Fraser 1965) is due to the omission of the positronium channel. It is noticeable that the importance of the positronium channel decreases as the angular momentum increases. The further improvement in the phase shifts for the more sophisticated $CC(\bar{28}, 3)$ model is relatively minor.

Table 1. Phase shifts (in rad) for positron-hydrogen scattering at an incident positron momentum of $0.5 a_0^{-1}$

Method	$J = 0$	$J = 1$	$J = 2$	$J = 3$
$CC(\bar{28}, 0)$	-0.00462	0.0949	0.0328	0.0117
$CC(\bar{28}, 1)$	0.0535	0.1275	0.0389	0.0123
$CC(\bar{28}, 3)$	0.0540	0.1289	0.0391	0.0124
$CC(\bar{6}, \bar{6})$	0.0536	0.1267	0.0386	0.0124
$CC(\bar{13}, \bar{8})$	0.0621	0.1306	0.0397	0.0126
Variational ^A	0.0624	0.1309		

^A Variational method (Bhatia *et al.* 1971, 1974).

It can be seen from Table 2 that the $CC(\bar{28}, 0)$ model does not predict the elastic cross section at $E = 0.64$ Ryd with any accuracy. The integrated cross section is only half of that predicted by the $CC(\bar{13}, \bar{8})$ model. The inclusion of a single positronium state results in the $CC(\bar{28}, 1)$ model giving an integrated cross section that is only 5% smaller than the $CC(\bar{13}, \bar{8})$ cross section. The more sophisticated $CC(\bar{28}, 3)$ model is only marginally better than the $CC(\bar{28}, 1)$ model. When it comes to the prediction of the positronium formation cross section, both the $CC(\bar{28}, 1)$ and $CC(\bar{28}, 3)$ models give integrated cross sections within 6% of the best calculation, with the $CC(\bar{28}, 3)$ model being accurate to within 3%.

Since the $CC(\bar{13}, \bar{8})$ cross sections are expected to be within 2% of the exact cross section, the agreement indicates that the present model is able to reproduce both the integrated elastic and positronium cross sections in the low energy region with an error of about 5%.

It is also instructive to compare results at 1.0 Ryd, which is the highest energy for which $CC(\bar{13}, \bar{8})$ cross sections were computed. Cross sections are listed in Table 3. The present $CC(\bar{28}, 3)$ model gives 1.034 and 3.26 πa_0^2 for the elastic and $Ps(1s)$ formation cross sections respectively. These cross sections compare well with the $CC(\bar{13}, \bar{8})$ cross sections of 1.07 and 3.40 πa_0^2 respectively. Apart from the weak transitions to the $Ps(2s)$ and $Ps(2p)$ states, the two sets of cross sections agree to within 5%. The inclusion of the $Ps(2s)$ and $Ps(2p)$ levels in the CC expansion is mainly important for the total Ps formation cross section. The

$CC(\overline{28}, 1)$ model gives $3.167 \pi a_0^2$ for the $Ps(1s)$ formation cross sections which is $0.1 \pi a_0^2$ smaller than the $CC(\overline{28}, 3)$ cross section. The differences between the $CC(\overline{28}, 1)$ and $CC(\overline{28}, 3)$ results are much smaller for the elastic cross section and the $H(2s)$ and $H(2p)$ excitation cross sections.

Table 2. The $J = 0, 1, 2$ partial and integrated cross sections (in πa_0^2) for elastic scattering and positronium formation at $E = 0.64$ Ryd

Method	$J = 0$	$J = 1$	$J = 2$	Summed
<i>Elastic</i>				
$CC(\overline{28}, 0)$	0.133	0.288	0.201	0.690
$CC(\overline{28}, 1)$	0.0775	0.602	0.468	1.27
$CC(\overline{28}, 3)$	0.0767	0.603	0.477	1.28
$CC(\overline{6}, \overline{6})$	0.0730	0.589	0.455	1.25
$CC(\overline{9}, \overline{9})$	0.071	0.624	0.482	
$CC(\overline{13}, \overline{8})$	0.0657	0.626	0.484	1.32
Variational ^A	0.065	0.622	0.423	
<i>Ps formation</i>				
$CC(\overline{28}, 1)$	0.396^{-2}	0.482	0.834	1.59
$CC(\overline{28}, 3)$	0.429^{-2}	0.477	0.840	1.62
$CC(\overline{6}, \overline{6})$	0.439^{-2}	0.484	0.841	1.64
$CC(\overline{9}, \overline{9})$	0.41^{-2}	0.485	0.871	
$CC(\overline{13}, \overline{8})$	0.472^{-2}	0.483	0.859	1.66
Variational ^A	0.49^{-2}	0.482	0.812	

^A Kohn-variational (Brown and Humberston 1985; Humberston 1982, 1984).

Table 3. The integrated cross sections (in πa_0^2) for positron-hydrogen scattering at $E = 1.0$ Ryd

Method	Elastic	$Ps(1s)$	$H(2s)$	$H(2p)$	$Ps(2s)$	$Ps(2p)$
$CC(\overline{13}, \overline{8})$	1.068	3.397	0.284	0.420	0.0266	0.0328
$CC(\overline{28}, 0)$	0.753		0.520	0.622		
$CC(\overline{28}, 1)$	1.017	3.167	0.304	0.410		
$CC(\overline{28}, 3)$	1.034	3.261	0.301	0.403	0.0222	0.0262

4. Cross Sections

(4a) Elastic Scattering

The integrated cross section for elastic scattering is shown in Fig. 1 and compared with other results. An indication of the accuracy of the present calculation is provided by the size of the discontinuity between the $CC(\overline{13}, \overline{8})$ and $CC(\overline{28}, 3)$ cross sections at the common energy of 1.0 Ryd. Since the $CC(\overline{13}, \overline{8})$ calculation is expected to have an accuracy of about 2%, it is clear from the small size of the discontinuity that the $CC(\overline{28}, 3)$ cross sections have an accuracy of better than 10% at 1.0 Ryd. One of the more interesting features of this graph is the manner in which the $CC(\overline{28}, 3)$ and $CC(\overline{28}, 0)$ cross sections converge towards each other as the energy increases.

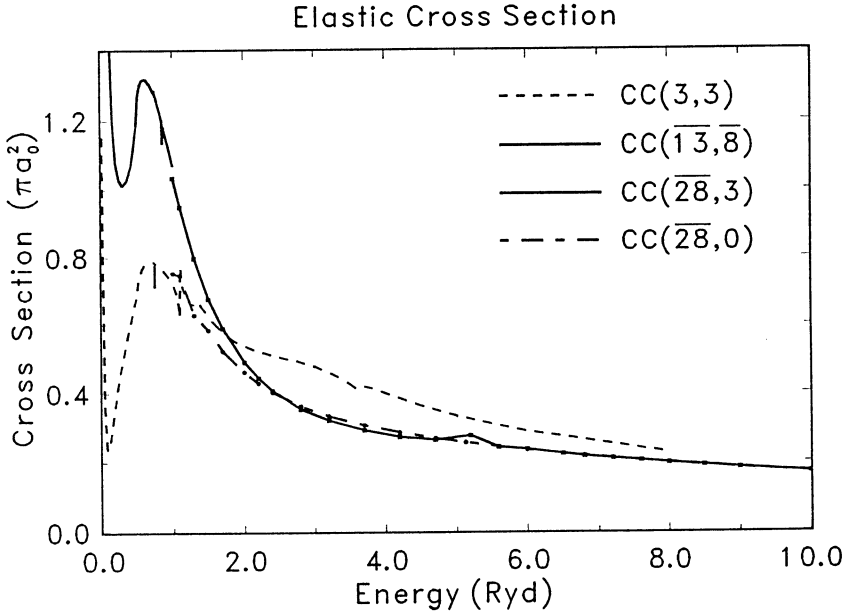


Fig. 1. Elastic cross section (in πa_0^2) for positron-hydrogen scattering. The $CC(\overline{13}, \overline{8})$ cross section (solid line) is shown for $E < 1.0$ Ryd. The $CC(\overline{28}, \overline{0})$ (alternating long and short dashes) and $CC(\overline{28}, \overline{3})$ (solid line) cross sections are shown for $E > 1.0$ Ryd. The $CC(3,3)$ cross section is shown for all energies (short dashes).

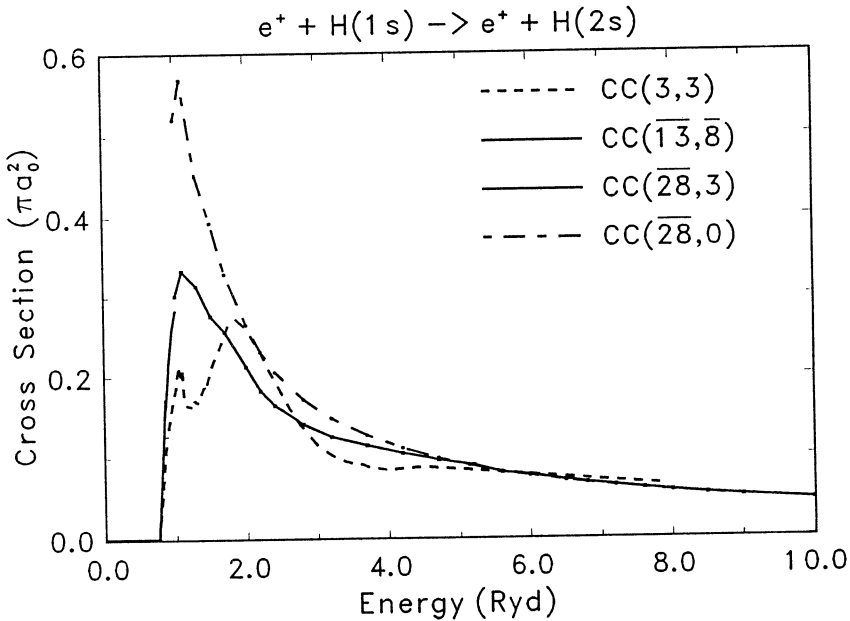


Fig. 2. Cross sections (in πa_0^2) for excitation of the $H(2s)$ state. The $CC(\overline{13}, \overline{8})$ (solid line) cross section is shown for $E < 1.0$ Ryd and the $CC(\overline{28}, \overline{0})$ (alternating long and short dashes) and $CC(\overline{28}, \overline{3})$ (solid line) cross sections are shown for $E > 1.0$ Ryd. Also shown is the $CC(3,3)$ (short dashes) cross section.

The most accurate of the recent single-centre calculations is probably the IERM calculation. Despite its name, the convergent close coupling calculation (Bray and Stelbovics 1994) only included L^2 states with $l \leq 3$ and is unlikely to converge. Evidence from the IERM calculation (Higgins *et al.* 1990) suggests that the CC expansion should include L^2 pseudo-states with at least $l = 4$ for the elastic T -matrix to be close to convergence. Cross sections from these other sources are not shown in Fig. 1 since they are all roughly the same size for energies greater than 3 Ryd and their inclusion would only give the figure a cluttered appearance.

An irregularity in the $CC(\overline{28}, 3)$ cross section is evident near 5 Ryd. Fluctuations are also present in some of the other transitions; most noticeably the ionisation cross section depicted in Fig. 5. Given the time-consuming nature of the $CC(\overline{28}, 3)$ calculations, it was not possible to obtain a detailed map of these fluctuations on a fine energy grid. At some of the energies the calculations were repeated with different discretisations of the integral equation with no major change in the cross sections. Therefore the fluctuations cannot be ascribed to a numerical artefact. Examination of the $J = 0$ and $J = 1$ partial cross sections seems to indicate the presence of resonant structures similar to those seen in previous calculations (Higgins and Burke 1991; McAlinden *et al.* 1994; Mitroy *et al.* 1994). It has been suggested that these structures are artefacts of calculations that do not properly incorporate the positron–hydrogen ionisation continuum (Kernoghan *et al.* 1994).

(4b) Excitation of the $H(2s)$ Level

The integrated cross section for the positron impact excitation of the $H(2s)$ state is shown in Fig. 2. Once again, the $CC(\overline{28}, 3)$ and $CC(\overline{28}, 0)$ cross sections converge towards each other as the energy increases. At energies greater than 5 Ryd, the two cross sections are the same for all practical purposes.

(4c) Excitation of the $H(2p)$ Level

The integrated cross section for the positron impact excitation of the $H(2p)$ state is shown in Fig. 3. The $CC(\overline{28}, 3)$ and $CC(\overline{28}, 0)$ cross sections converge towards each other and are essentially the same when $E > 5$ Ryd. At the highest energies, the $CC(3, 3)$ cross section is clearly different from the $CC(\overline{28}, 3)$ cross section. One interpretation of this is that coupling to the ionisation continuum is more important than coupling to the positronium channels at the higher energies. This suggestion is supported by the respective sizes of the total Ps formation and ionisation cross sections which are about $0.02 \pi a_0^2$ and $0.74 \pi a_0^2$ respectively at an energy of 8 Ryd. A similar trend for the $CC(\overline{28}, 0)$ and $CC(\overline{28}, 3)$ cross sections to converge to each other and not to the $CC(3, 3)$ cross section is also present for the elastic and $H(2s)$ cross sections.

One of the salient features of Fig. 3 is the shoulder in the $CC(\overline{28}, 3)$ cross section at about 1.3 Ryd. A similar structure is even more prominent in the $CC(3, 3)$ cross section. Whether such a structure is a real feature of the positron–hydrogen spectrum is obviously an interesting question. Besides performing an experiment, another way to resolve the question would be to perform another calculation of the present type to see whether the size of the bump decreases as the dimension of the L^2 basis is increased.

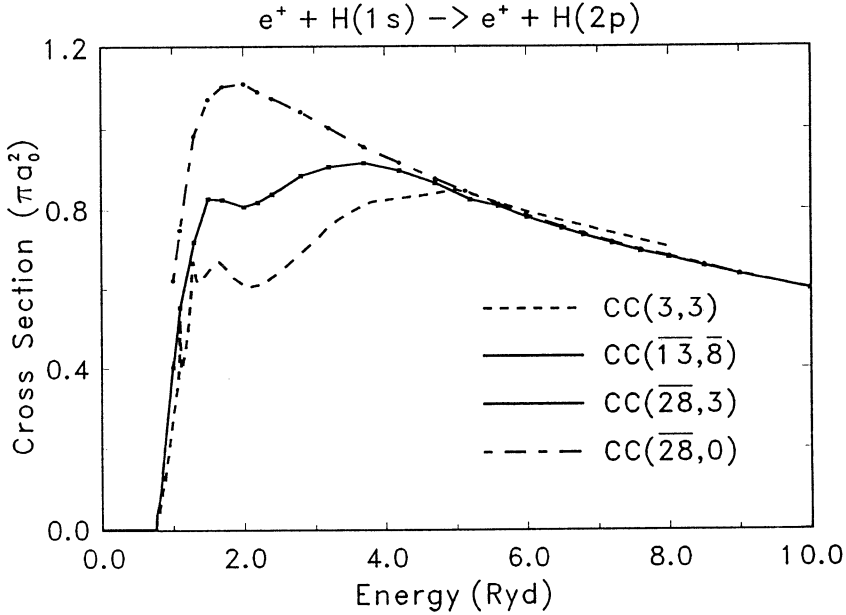


Fig. 3. Cross sections (in πa_0^2) for excitation of the $H(2p)$ level. The $CC(\overline{13}, \overline{8})$ (solid line) cross section is shown for $E < 1.0$ Ryd and the $CC(\overline{28}, 0)$ (alternating long and short dashes) and $CC(\overline{28}, \overline{3})$ (solid line) cross sections are shown for $E > 1.0$ Ryd. Also shown is the $CC(\overline{3}, \overline{3})$ cross section (short dashes).

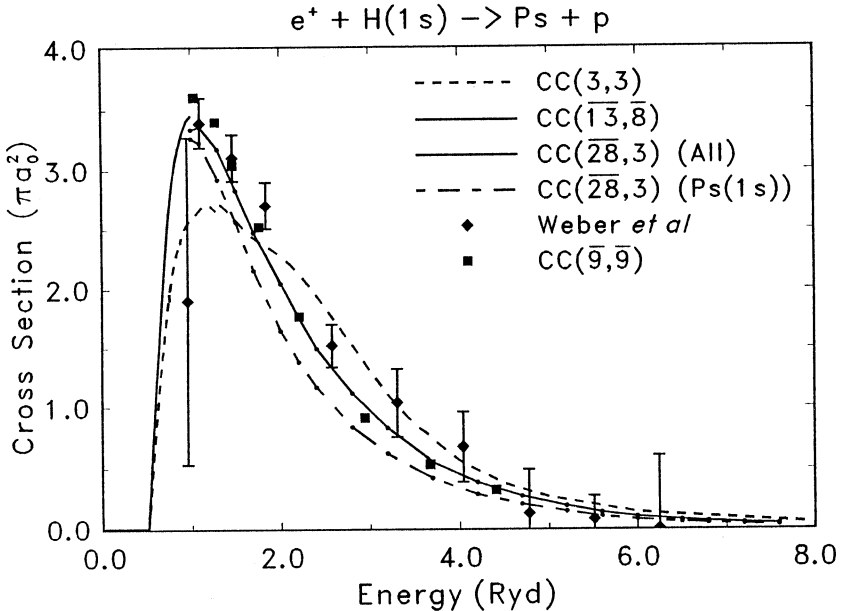


Fig. 4. Net positronium formation cross section (in πa_0^2) for positron-hydrogen scattering. The $CC(\overline{13}, \overline{8})$ (solid line) cross section is shown for $E < 1.0$ Ryd. The $CC(\overline{3}, \overline{3})$ cross section (short dashes) represents the sum of the $Ps(1s)$, $Ps(2s)$, and $Ps(2p)$ cross sections. The $CC(\overline{28}, \overline{3})$ cross section for $Ps(1s)$ formation (alternating dashes) and the $CC(\overline{28}, \overline{3})$ cross section for Ps formation in all levels (solid line) are shown for $E > 1.0$ Ryd. The net positronium cross section from the R -matrix calculation is also shown (squares) at a discrete number of points. The experimental data are from the Bielefeld-Brookhaven experiment (diamonds).

(4d) Positronium Formation

In Fig. 4, the positronium formation cross sections computed in a variety of different models are compared with the experimental data of the Bielefeld-Brookhaven collaboration (Sperber *et al.* 1992; Weber *et al.* 1994). Two sets of $CC(\bar{28}, 3)$ cross sections are depicted. The first shows the cross section for positronium formation in the $Ps(1s)$ ground state. The other cross section includes contributions from the $Ps(n \geq 2)$ states. The actual expression used to compute the total positronium cross section is

$$\sigma_{total,Ps} = \sigma_{Ps(1s)} + 1.6(\sigma_{Ps(2s)} + \sigma_{Ps(2p)}).$$

The factor of 1.6 arises from assuming a $1/n^3$ scaling for positronium formation in the $n \geq 3$ levels. It is easily seen from Fig. 4 that the $Ps(n=2)$ and higher levels make a significant contribution to the total positronium formation cross section. At most energies, these levels contribute about 30% to the net Ps formation cross section.

Once again, an indication of the accuracy of the present calculation is provided by the size of the discontinuity between the $CC(\bar{13}, \bar{8})$ cross section and $CC(\bar{28}, 3)$ cross sections at an energy of 1.0 Ryd. The size of the discontinuity is about $0.1 \pi a_0^2$. It is also noticeable that the $CC(\bar{9}, \bar{9})$ cross section is larger than the $CC(\bar{13}, \bar{8})$ cross section by about $0.1 \pi a_0^2$ at this energy. While the difference between the $CC(\bar{13}, \bar{8})$ and $CC(\bar{28}, 3)$ cross sections is due to model-dependent features, it is not clear whether part of the difference between the $CC(\bar{13}, \bar{8})$ and $CC(\bar{9}, \bar{9})$ cross sections might not be due to numerical factors. Comparisons of a sequence of different model calculations at low energies (Mitroy 1995) reveal that the trend is for the positronium formation cross section to increase as the sophistication of the model is increased. Therefore, the fact that the $CC(\bar{9}, \bar{9})$ cross section is larger than the $CC(\bar{13}, \bar{8})$ cross section does seem unusual and it is possible that numerical inaccuracies may be leading to the $CC(\bar{9}, \bar{9})$ cross section being too large by $0.1-0.2 \pi a_0^2$.

Close to the ionisation threshold, the $CC(\bar{28}, 3)$ cross section is larger than the $CC(3, 3)$ cross section and in closer agreement with experiment near the cross section maximum. However, the $CC(\bar{28}, 3)$ cross section decreases more rapidly than the $CC(3, 3)$ cross section and at an energy of 2.0 Ryd is smaller than the $CC(3, 3)$ cross section. At these higher energies, experimental uncertainties associated with discriminating between ionisation and positronium formation are large and for all practical purposes both the $CC(\bar{28}, 3)$ and $CC(3, 3)$ models provide an equally good fit to the data. The energy dependence of the $CC(\bar{28}, 3)$ cross section and the $CC(\bar{9}, \bar{9})$ cross section computed with the R -matrix method are very similar [the data for the R -matrix cross section are interpolated from the curve in Fig. 4 of Kernoghan *et al.* (1995), which presumably uses the same $1/n^3$ extrapolation]. The $CC(\bar{9}, \bar{9})$ cross section is some 5% larger at the lower energies, although the extent to which this might be a numerical artefact needs clarification.

It is worth noting that the bump present in the Ps formation at 2 Ryd for the $CC(3, 3)$ model is absent in the present calculation. All the low- J partial cross sections in the $CC(3, 3)$ model have a definite bump near 2 Ryd (McAlinden *et al.* 1994; Mitroy and Stelbovics 1994b). An examination of the partial cross

sections for the $CC(\overline{28}, 3)$ model did not reveal any structures near 2 Ryd. It had been suggested (Kernoghan *et al.* 1994) that these bumps might arise from the positronium channels acting as a conduit for flux destined for the ionisation channels. The present results are consistent with this hypothesis.

One of the other salient features of Fig. 4 is the rate at which the Ps formation cross section decreases at high energy. The Ps formation decreases more rapidly than any of the other cross sections shown in the other figures, and at an energy of 9.0 Ryd the summed Ps formation cross section is only $0.0169 \pi a_0^2$.

(4e) Ionisation

The ionisation cross section is computed from the individual pseudo-state cross sections by adding them up with a small correction for some of the pseudo-states. To be specific, the ionisation cross section is computed from the manifold of $e^+ - H$ channels using

$$\sigma_I = \sum_{\alpha} \sigma_{\alpha} \left(1 - \sum_i \langle \psi_i | \psi_{\alpha} \rangle^2 \right),$$

where the ψ_i are the exact hydrogenic states and ψ_{α} are the L^2 pseudo-states. The correction for the non-zero overlap is only performed for the negative energy pseudo-states in the L^2 manifold of hydrogen states.

The cross sections are compared with experiment, and with other calculations, in Fig. 5. Two separate experiments have reported ionisation cross sections (Jones *et al.* 1993; Spicher *et al.* 1990). There are large discrepancies between the two sets of experimental data. The results of the University College London (UCL) group (Jones *et al.* 1993) should be preferred to those of the Bielefeld group (Spicher *et al.* 1990) since those of the UCL group merge with the electron-hydrogen ionisation cross sections for $E > 8$ Ryd. Besides the calculations with which direct comparisons have been made, the ionisation cross section for positron-hydrogen scattering has also been computed in a distorted wave approximation (Acacia *et al.* 1993, 1994). These cross sections are only likely to be accurate for $E > 100$ eV and therefore no explicit comparison is made.

The agreement of the present $CC(\overline{28}, 3)$ ionisation cross section with the experimental data of the UCL group could scarcely be any better. The experimental ionisation cross section has a somewhat unusual shape. It attains its maximum value close to 2.5 Ryd, and thereafter the decrease in the cross section is very slow. Indeed, the cross section is almost constant over the entire energy range from 2.5 to 9 Ryd. The $CC(\overline{28}, 3)$ model cross section is also very flat over this energy range. The $CC(\overline{28}, 0)$ model has a different shape, with a pronounced peak near 2.3 Ryd. The $CC(\overline{28}, 0)$ model is probably nowhere near the convergence limit for a single-centre calculation. The peak cross section for the CCC calculation (Bray and Stelbovics 1994) which included $l = 3$ pseudo-states is almost $2.25 \pi a_0^2$, which is about $0.6 \pi a_0^2$ larger than the present cross section peak. The big difference between the two cross sections would seem to indicate that a converged single-centre calculation should include at least $l = 4$ pseudo-states in the basis.

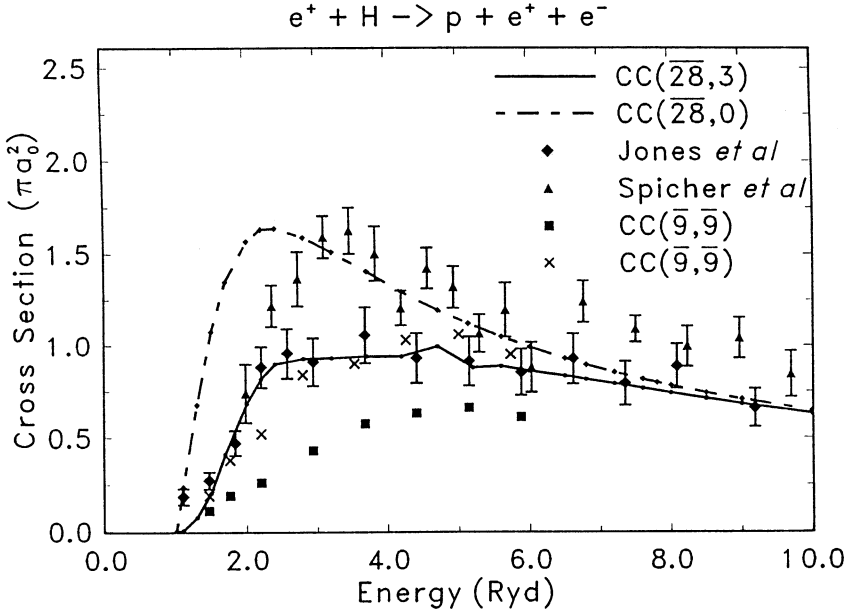


Fig. 5. The ionisation cross section (in πa_0^2) for positron–hydrogen scattering. The $CC(\overline{28}, 0)$ (alternating dashes) and $CC(\overline{28}, \overline{3})$ (solid line) cross sections are shown. The experimental data from the UCL (diamonds) and Bielefeld (triangles) groups, and the R -matrix cross sections (squares $e^+ - H$ channels only, crosses $e^+ - H$ and $P_s - p$ channels) are also shown at a discrete number of points.

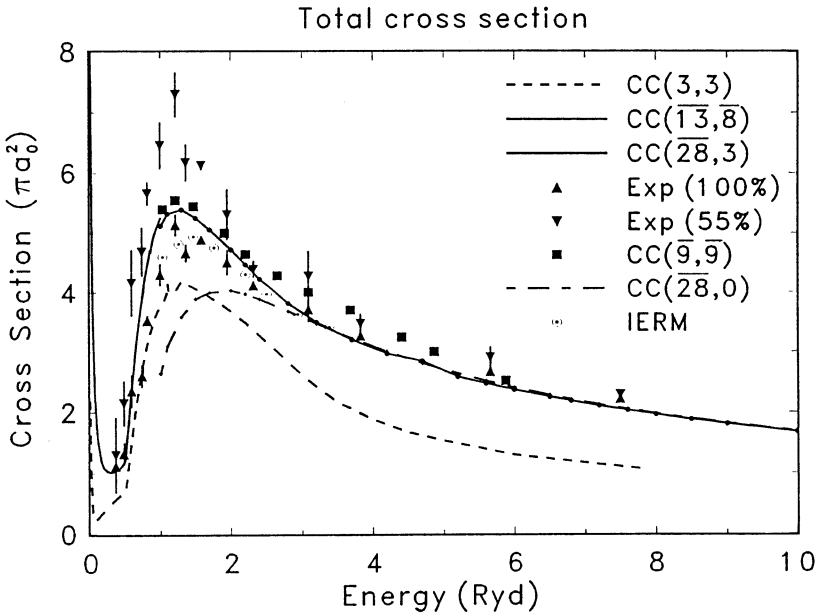


Fig. 6. Total reaction cross sections (in πa_0^2) for positron–hydrogen scattering. The $CC(\overline{13}, \overline{8})$ (solid line) cross section is shown for $E < 1.0$ Ryd. The $CC(\overline{28}, 0)$ (alternating dashes) and $CC(\overline{28}, \overline{3})$ (solid line) cross sections are shown for $E > 1.0$ Ryd. The cross sections for the $CC(3, 3)$ model (short dashes), IERM calculation (circles with dots) and $CC(\overline{9}, \overline{9})$ calculation (squares) are also shown. The experimental data of the Detroit group are based on either 100% dissociation (triangles pointing up) or 55% dissociation (triangles pointing down).

The manner in which the $CC(\bar{28}, 0)$ and $CC(\bar{28}, 3)$ ionisation cross sections approach each other as the energy increases is qualitatively different to the manner in which the model cross sections asymptote towards each other for the transitions to the $H(2s)$ and $H(2p)$ levels. For all practical purposes, the $CC(\bar{28}, 0)$ and $CC(\bar{28}, 3)$ integrated $H(2s)$ and $H(2p)$ cross sections were identical for $E > 5$ Ryd. The ionisation cross sections from the two models converge towards each other much more slowly and they only begin to merge at the highest energy, namely $E = 10$ Ryd. Since ionisation and positronium formation both involve the removal of the electron from the hydrogen atom, it is not surprising that the coupling between the positronium states and the ionisation continuum seems to be stronger than the coupling between the positronium states and the bound hydrogen states.

One notable feature of Fig. 5 is the presence of fluctuations in the energy dependence of the ionisation cross sections near 5 Ryd. As discussed earlier, it seems likely that these fluctuations are due to resonant structures similar to those seen in previous calculations (McAlinden *et al.* 1994; Mitroy *et al.* 1994*b*). It is probable that these structures do not represent real features in the cross section (Kernoghan *et al.* 1994).

The interpretation of the $CC(\bar{9}, \bar{9})$ R -matrix cross sections of Kernoghan *et al.* (1995) is more problematic. They present two different versions of the ionisation cross section. One version is determined by adding the $e^+ - H$ pseudo-state excitation cross sections (after correcting for bound state overlaps). They also computed the ionisation cross section by adding the pseudo-state excitation cross sections for *both* the $e^+ - H$ and $Ps - p$ groups of channels. The cross section computed using both manifolds of channels was in better agreement with experiment. However, including cross sections from both manifolds of channels immediately raises the spectre of 'double counting'. The $CC(\bar{9}, \bar{9})$ basis is unlikely to give a good representation of the positron-hydrogen continuum due to the limited number of positron-hydrogen channels. Therefore, it is unlikely that the cross sections computed from just the $e^+ - H$ manifold of channels will be anywhere close to converged. If this is the case, then it is to be expected that the ionisation cross section computed from the $e^+ - H$ pseudo-state excitation cross sections would underestimate the experimental cross section and this is seen to be the case from Fig. 5. Under these circumstances, the fact that the cross section computed by adding the cross sections from both the $e^+ - H$ and $Ps - p$ manifolds is larger and happens to agree better with experiment could be nothing more than a numerical coincidence. It would be instructive to perform a larger calculation of this type, say with a $CC(\bar{12}, \bar{12})$ basis, to determine whether the cross section calculated from both manifolds of channels would begin to overestimate the experimental ionisation cross section.

(4f) Total Reaction Cross Section

The total reaction cross section for both the $CC(\bar{28}, 3)$ and $CC(\bar{28}, 0)$ models is computed by summing all the individual cross sections. The small correction arising from Ps formation in states with $n \geq 3$ is also included in the total reaction cross section for the $CC(\bar{28}, 3)$ model.

Once again, it is easily seen from Fig. 6 that the single-centre $CC(\bar{28}, 0)$ model gives an inadequate description of positron-hydrogen scattering. At incident energies less than 2 Ryd, the $CC(\bar{28}, 0)$ cross section is much smaller than the

IERM cross section. However, as the energy increases, the $CC(\bar{28}, 0)$ begins to asymptote towards the IERM cross section. The need to include a large number of partial waves in the pseudo-state basis has been attributed to the need to provide a representation of virtual and real positronium channels during the collision. Therefore, as the energy increases and the possibility of positronium formation diminishes rapidly, it is to be expected that the necessity of having a large number of partial waves in the L^2 basis should also decrease in importance. Although the CCC calculation is not shown in Fig. 6, similar considerations are important. The CCC cross section is significantly smaller than the IERM cross section for $E < 2$ Ryd, and is much closer to the IERM at the higher energies.

The total reaction cross section has been measured by the Detroit group (Zhou *et al.* 1994). The experimental cross sections do not discriminate against small-angle elastic scattering and could therefore underestimate the actual reaction cross section. They also report two sets of cross sections which depend on the efficiency with which the H_2 molecules undergo dissociation into atomic H (results are reported assuming a 55% or 100% dissociation efficiency). The experimental data are able to expose inadequacies in the $CC(3, 3)$ model, which yields cross sections that are clearly incompatible with experiment. However, the large uncertainties that surround this experiment do not make it possible to make precise statements about the accuracy of the more refined calculations. As far as we can tell from the comparison shown in Fig. 6, there are no significant disagreements between the present $CC(\bar{28}, 3)$ cross section and experiment.

The total cross section for the R -matrix $CC(\bar{9}, \bar{9})$ calculation is somewhat larger than the present cross section, with the difference being largest between 2 and 5 Ryd. Given the uncertainties present in the interpretation of the Ps-p pseudo-state cross sections, and whether these cross sections should be included in the evaluation of the total cross section, a difference between the two sets of cross sections is to be expected. Indeed, the difference between the two sets of cross sections seems to be roughly equal to the contribution to the cross section from the positronium pseudo-states.

5. Conclusion

To summarise, a model of positron-hydrogen scattering has been developed that is accurate to about 5% at low energies and should have an accuracy of about 10% at intermediate energies. The present cross sections are generally consistent with experimental ionisation, total reaction and positronium cross sections.

The largest discrepancy with experiment occurs for the positronium formation cross section between 1.5 and 2.5 Ryd. While comparisons with previous calculations at low energies suggest that the present positronium cross section may be too small by $0.1 \pi a_0^2$, an increase in the present positronium formation cross section by this amount might not be sufficient to give perfect agreement with experiment. It may be appropriate to perform further experiments in order to refine current estimates of the positronium formation cross section.

The biggest source of uncertainty in the calculation is probably the restriction of the L^2 pseudo-state basis to include states with $l \leq 2$. It is known from single-centre CC type calculations that the cross sections converge very slowly as the maximum angular momentum of the L^2 basis is increased. The slow convergence of the single-centre calculations is believed to be due to the omission

of positronium levels from the CC expansion. With no positronium levels included, the single-centre calculations would need a very large partial wave expansion to represent the correlations between the electron and positron close to the nucleus. The addition of just a single positronium state to a large single-centre CC expansion has been shown to dramatically increase the convergence of the cross sections at low energies.

At high energies, the coupling between the hydrogen and positronium channels becomes very weak, resulting in the merging of the $CC(\overline{28}, 0)$ and $CC(\overline{28}, 3)$ cross sections and a Ps formation cross section that is very small. For all practical purposes, it should be possible to omit the rearrangement channels from calculations of positron-hydrogen scattering as long as the incident positron energy is greater than 10 Ryd.

Unlike some previous calculations undertaken at low energies (Mitroy 1995), the present work was not intended to be an exhaustive calculation. The aim of this calculation has been to demonstrate that the addition of a few positronium states to a large L^2 basis of hydrogen states leads to a model that can describe most of the physics of positron-hydrogen collisions in the low and intermediate energy regions. It would certainly be interesting to increase the size of the L^2 basis to include states with $l = 3$ and repeat the present calculation, thereby gaining additional information regarding the convergence of the cross sections.

Acknowledgments

This research was supported by a large project grant from the Australian Research Council.

References

- Acacia, P., Campaneau, R. I., Horbatsch, M., McEachran, R. P., and Stauffer, A. D. (1993). *Phys. Lett. A* **179**, 205.
- Acacia, P., Campaneau, R. I., Horbatsch, M., McEachran, R. P., and Stauffer, A. D. (1994). *Hypf. Int. A* **89**, 95.
- Archer, B. J., Parker, G. A., and Pack, R. T. (1990). *Phys. Rev. A* **41**, 1303.
- Bhatia, A. K., Temkin, A., Drachman, R. J., and Eiserike, H. (1971). *Phys. Rev. A* **3**, 1328.
- Bhatia, A. K., Temkin, A., and Eiserike, H. (1974). *Phys. Rev. A* **9**, 219.
- Bransden, B. H., and Noble, C. J. (1994). *Adv. At. Mol. Opt. Phys.* **32**, 19.
- Bray, I., and Stelbovics, A. T. (1992). *Phys. Rev. A* **46**, 6995.
- Bray, I., and Stelbovics, A. T. (1993). *Phys. Rev. Lett.* **70**, 746.
- Bray, I., and Stelbovics, A. T. (1994). *Phys. Rev. A* **49**, R2224.
- Brown, C. J., and Humberston, J. W. (1985). *J. Phys. B* **18**, L401.
- Drake, G. W. F. (1993). In 'Long-Range Casimir Forces' (Eds F. S. Levin and D. A. Micha), p. 107 (Plenum: New York).
- Hewitt, R. N., Noble, C. J., and Bransden, B. H. (1990). *J. Phys. B* **23**, 4185.
- Higgins, K., Burke, P. G., and Walters, H. R. J. (1990). *J. Phys. B* **23**, 1345.
- Higgins, K., and Burke, P. G. (1991). *J. Phys. B* **21**, L343-9.
- Humberston, J. W. (1982). *Can. J. Phys.* **60**, 591.
- Humberston, J. W. (1984). *J. Phys. B* **17**, 2353.
- Igarashi, A. and Toshima, N. (1994). *Phys. Rev. A* **50**, 232.
- Jones, G. O., Charlton, M., Slevin, J., Larricchia, G., Kover, A., Poulsen, M. R., and Nic Chormaic, S. (1993). *J. Phys. B* **26**, L483.
- Kernoghan, A. A., McAlinden, M. T., and Walters, H. R. J. (1994). *J. Phys. B* **27**, L543.
- Kernoghan, A. A., McAlinden, M. T., and Walters, H. R. J. (1995). *J. Phys. B* **28**, 1079.
- McAlinden, M. T., Kernoghan, A. A., and Walters, H. R. J. (1994). *Hypf. Int.* **89**, 161.

- McCarthy, I. E., and Stelbovics, A. T. (1983). *Phys. Rev. A* **28**, 2693.
- McEachran, R. P., and Fraser, P. (1965). *Proc. Phys. Soc. London B* **6**, 369.
- Mitroy, J. (1993a). *Aust. J. Phys.* **46**, 751.
- Mitroy, J. (1993b). *J. Phys. B* **26**, 4861.
- Mitroy, J. (1995). *Aust. J. Phys.* **48**, 646.
- Mitroy, J. (1996). *J. Phys. B* **29**, L263.
- Mitroy, J., and Ratnavelu, K. (1995). *J. Phys. B* **28**, 287.
- Mitroy, J., and Stelbovics, A. T. (1994a). *J. Phys. B* **27**, L55.
- Mitroy, J., and Stelbovics, A. T. (1994b). *J. Phys. B* **27**, 3257.
- Mitroy, J., and Stelbovics, A. T. (1994c). *Phys. Rev. Lett.* **72**, 3495.
- Mitroy, J., Berge, L., and Stelbovics, A. T. (1994). *Phys. Rev. Lett.* **73**, 2966.
- Pekeris, C. L. (1959). *Phys. Rev.* **115**, 1216.
- Sarkar, N. K., and Ghosh, A. S. (1994). *J. Phys. B* **27**, 759.
- Sperber, W., Becker, D., Lynn, K. G., Raith, W., Schwab, A., Sinapius, G., Spicher, G., and Weber, M. (1992). *Phys. Rev. Lett.* **68**, 3690.
- Spicher, G., Olsson, B., Raith, W., Sinapius, G., and Sperber, W. (1990). *Phys. Rev. Lett.* **64**, 1019.
- Stelbovics, A. T., and Berge, L. (1996). *Aust. J. Phys.* **49**, 273.
- Walters, H. R. J. (1988). *J. Phys. B* **21**, 1893.
- Weber, M., Hofmann, A., Raith, W., Sperber, W., Jacobsen, F., and Lynn, K. G. (1994). *Hypf. Int.* **89**, 221.
- Winick, J. R., and Reinhardt, W. P. (1978a). *Phys. Rev. A* **18**, 910.
- Winick, J. R., and Reinhardt, W. P. (1978b). *Phys. Rev. A* **18**, 925.
- Zhou, S., Kauppila, W. E., Kwan, C. K., and Stein, T. S. (1994). *Phys. Rev. Lett.* **72**, 1443.
- Zhou, Y., and Lin, C. D. (1994). *J. Phys. B* **27**, 5065.
- Zhou, Y., and Lin, C. D. (1995). *J. Phys. B* **28**, 4907.